Study on the structure and properties of EVA/clay nanocomposites

YAN TIAN, HUI YU, SHISHAN WU*, GENDING JI
College of Chemistry and Chemical Engineering, Nanjing University, Nanjing 210093, People's Republic of China
E-mail: shshwu@sina.com

JIAN SHEN
College of Chemistry and Chemical Engineering, Nanjing University, Nanjing 210093, People's Republic of China; College of Chemistry and Environment Science, Nanjing Normal University, Nanjing 210097, People's Republic of China

In recent years, the study of polymer-layered silicate nanocomposites (PLSN) has attracted great interest since they exhibit unexpected hybrid properties synergistically derived from two components. Compared to conventionally filled microcomposites, PLSN typically exhibit increased modulus, strength and heat distortion temperature [1–3], good barrier properties [4–6], reduced flammability [7], and improved ablative performance [8], due to their nanoscale structure. Thus they open up new technological and economic perspectives. Poly(ethylene-co-vinylacetate) (EVA) is a relatively widely used copolymer, for example, as a modifier for wax and other systems, in hot-melt-adhesives, and in the electrical cable sheathing industry. In 2001, Zanetti *et al.* [9–13] have reported the results on the structure and thermal behavior of EVA-layered silicate nanocomposites. This paper describes the structure and the mechanical and thermal properties of EVA/clay nanocomposites based on montmorillonite.

The poly(ethylene-co-vinylacetate) (EVA) with 28 wt% of vinylacetate used to prepare the composites was Escogene UL 150/28 produced by Exxon. The Ca-montmorillonite (MMT) used to prepare the composites was a natural clay mineral with a cation exchange capacity (CEC) of 100 mequiv/100 g, and the mean size of the clay particles was 40 μm. The cation exchange was carried out with octadecylammonium (ODA). In a 5000 mL three-necked flask were placed 240 g of octadecylamine, 1500 mL of alcohol, and 91 g of 36 wt% hydrochloric acid. This solution was heated to 80 °C. In 1500 mL of water, 150 g of montmorillonite (MMT) was dispersed at 80 °C. The dispersed solution was added to the solution of ammonium salt of octadecylamine, and this mixture was stirred vigorously for 8 h. A white precipitate was isolated by filtration, placed in a 5000 mL beaker with 3500 mL of hot alcohol-water solution, and stirred for 40 min. This process was repeated 5 times to remove the residue of ammonium salt of octadecylamine. The product was filtered and thoroughly dried in a vacuum oven, then ground into the size of 40 μm. This organic-montmorillonite was termed ODA-MMT. The EVA and filler were mixed in a twin-roll mill at a temperature of 120–125 °C for 10 min. The composites were then pressed using a hydraulic press at 110 °C for 10 min, and allowed to cool to room temperature in the ambient as the pressure was kept constant, and sheets were obtained.

Fourier transform infrared spectroscopy (FT-IR) analyses were carried out using a VECTOR22 spectrometer. X-ray diffraction (XRD) measurements were made directly from MMT and ODA-MMT powders. In the case of nanocomposites, the measurements were carried out on sheets. All these experiments were performed using a D/Max-RA X-ray diffractometer at a scan rate of 1.0 degree/min. The CuKα radiation source was operated at 40 kV and 100 mA. The tensile strength, Young's modulus and tear strength tests were performed according to the respective standards using an INSTRON 4466 tensile tester. Molau test: 0.6 g EVA/MMT or EVA/ODA-MMT composites were dissolved in 8 mL xylene and the solution was laid for 72 h, and observed in the solution state. The thermogravimetry (TG) analyses were carried out in nitrogen or air (80 cm^3/min) on a TA2100-SDT2960 thermobalance using 8–10 mg samples, heated from room temperature to 700 °C at 10 °C /min. The temperature of weight loss was termed T^i. The temperature corresponding to the maximum speed of weight loss was termed T^{max}.

The FT-IR spectra of clay and organoclay are shown in Fig. 1. They appear as a few of the new absorption bands around 3253, 2921, 2851 and 1469 cm^{-1} in FT-IR spectrum of the organoclay compared with clay. The present absorption bands at 2921 and 2851 cm^{-1} correspond to the asymmetric and symmetric stretching vibration of C–H bond ($-CH_3$ and $-CH_2$). The absorption peaks at 1469 and 3253 cm^{-1} corresponds to methylene's bending vibration and stretching vibration of N–H bond, respectively. The FT-IR results indicate that the octadecylammonium salt has been exchanged into the galleries of the silicate layers by cation exchange reaction.

As shown in Fig. 2, the diffraction peaks of the clay and organoclay appear around 5.9° and 4.4°, respectively, corresponding to the interlayer spacing of 1.50 and 2.01 nm, respectively. The interlayer spacing of the organoclay was expanded, which also suggests that the

*Author to whom all correspondence should be addressed.

0022–2461

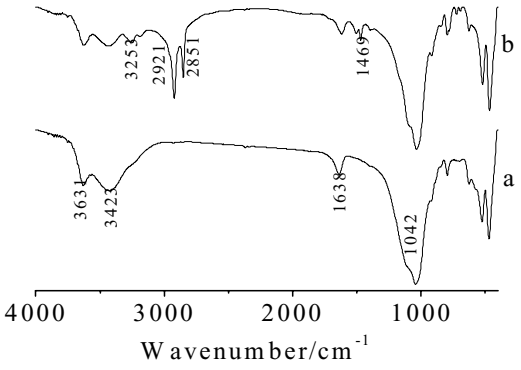

Figure 1 FT-IR spectra for (a) pure MMT and (b) ODA-MMT.

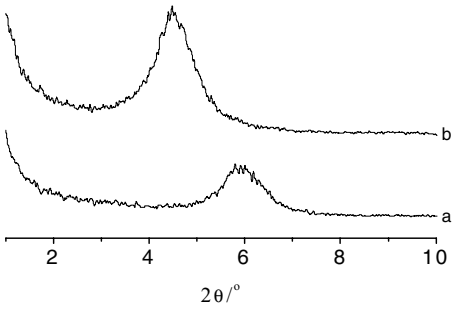

Figure 2 X-ray diffraction patterns for (a) pure MMT and (b) ODA-MMT.

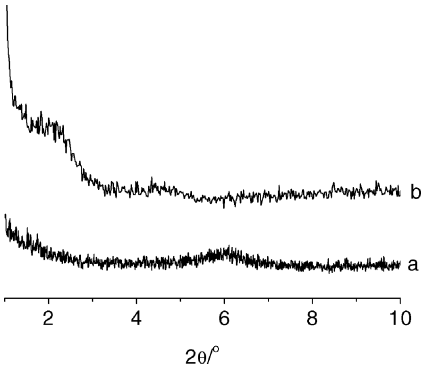

Figure 3 X-ray diffraction patterns for (a) EVA/MMT (95/5) composites obtained by blending 10 min and (b) EVA/ODA-MMT (95/5) composites obtained by blending 10 min.

octadecylammonium salt has intercalated into the galleries of silicate layers, in agreement with the above FT-IR results. Fig. 3 shows the XRD patterns for the EVA/clay (95/5) and EVA/organoclay (95/5) composites. The diffraction peak for the EVA/clay composite still appears at 5.9°, and the peak place is not removed, which indicates that the EVA chains did not intervene into the gallery of the layered silicates, and EVA/clay composites prepared by direct melt blending EVA and pristine clay were conventional particle-filled microcomposites. The diffraction peak for the EVA/organoclay composite appears around 2.0°, corresponding to interlayer spacing of 4.4 nm, which indicates that the EVA chains have intercalated into the gallery of the layered silicates. This illustrates that the silicate layers were uniformly dispersed in the EVA matrix in the nanometer and the intercalated EVA/organoclay nanocomposite were obtained. From

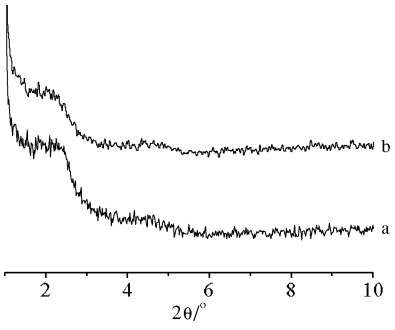

Figure 4 X-ray diffraction patterns for (a) EVA/ODA-MMT (95/5) obtained by blending for 10 min and (b) EVA/ODA-MMT (95/5) composites obtained by blending 15 min.

Fig. 4, we can see that all the diffraction peaks for EVA/organoclay (95/5) nanocomposite obtained after blending for 10 min and 15 min are around 2.0°, the silicate interlayer spacing dispersed in the EVA matrix was more enlarged with the blending time increasing, and thus blending time for 10 min is adequate for the preparation of EVA/organoclay nanocomposites.

Table I shows the mechanical properties of EVA/clay and EVA/organoclay composites. For the EVA/clay composites, the tensile and tear strength decreased with clay content increasing, the pristine clay could not stiffen the EVA materials. For the EVA/organoclay composites, the tensile and tear strength first increased with organoclay content increasing, and the best value is obtained at 5 wt% of organoclay content, and then decreased with further increased organoclay content due to the decrease in the degree of intercalation and dispersion of the silicate layers in the EVA matrix. The modulus of the two composites increases with the filler content increasing, but the increased degree for the EVA/organoclay composites is larger than that of EVA/clay composites. Compared with the EVA/clay (95/5) composites, the mechanical properties of the EVA/organoclay (95/5) nanocomposites are observably improved due to the nanoscale structure and strong interface interaction between the silicate layers and the EVA matrix. Table II data shows that EVA/organoclay composite obtained by blending for 10 min has the optimum tensile and tear strength, and then the tensile and tear strength decreased with further increased blending time due to degradation of the EVA chains.

The xylene solution of the EVA/clay (95/5) composites is separated into two parts of a transparent solution

TABLE I Mechanical properties of EVA, EVA/MMT and EVA/ODA-MMT composites obtained by blending for 10 min

Sample	Tensile strength (MPa)	Young's modulus (MPa)	Tear strength (MPa)
EVA	9.2	16.6	53.5
EVA/MMT (97/3)	8.9	17.0	54.6
EVA/MMT (95/5)	8.8	17.3	53.3
EVA/MMT (90/10)	7.3	18.2	48.1
EVA/ODA-MMT (97/3)	9.9	19.6	59.8
EVA/ODA-MMT (95/5)	10.5	21.5	62.4
EVA/ODA-MMT (90/10)	8.1	26.1	53.3

TABLE II Effects of blending time on the mechanical properties of EVA/MMT and EVA/ODA-MMT (95/5) composites

Sample	Blending time (min)	Tensile strength (MPa)	Young's modulus (MPa)	Tear strength (MPa)
EVA/ODA-MMT	5	9.5	20.1	58.5
EVA/ODA-MMT	10	10.5	21.5	62.4
EVA/ODA-MMT	15	9.9	25.2	61.1

TABLE III The TGA results of EVA, EVA/MMT (95/5) and EVA/ODA-MMT (95/5) composites in nitrogen

Sample	T_I^i (°C)	T_I^{max} (°C)	T_{II}^i (°C)	T_{II}^{max} (°C)
EVA	314	354	439	456
EVA/MMT	323	366	455	480
EVA/ODA-MMT	293	308	462	493

of EVA and clay deposit in the bottom of the test tube, indicating the weak interface interaction between the pristine clay and the EVA matrix. The xylene solution of the EVA/organoclay (95/5) nancomposites is uniformity in the emulsion, and the silicate layers can be suspended in the solution due to the dispersion of the silicate layers in the nanometer and strong interface interaction between the pristine clay and EVA matrix.

Table III shows the TGA results of EVA, EVA/clay and EVA/organoclay composites in nitrogen. In the first step, EVA/clay composite exhibited higher thermal stability than the pure EVA, whereas EVA/organoclay nanocomposite was degradated at a lower temperature than the pure EVA due to the acid catalysis of protonated silicate layers which formed the degradation of the octadecylammonium salt [10–12]. In the second step, the thermodegradation of EVA/organoclay nanocomposite took place at a higher temperature than EVA and EVA/clay composite due to the lower rate of the diffusion of the degradation products into the gas phase which caused the "labyrinth" effect of the silicate layers dispersed in the nanometer in the EVA matrix [10, 12].

The analyses carried out in air are reported in Table IV. During the first step, the thermal behavior of the EVA/organoclay nanocomposite in air was different in air with nitrogen, and no catalytic effect is observed, and its thermal stability was higher than the EVA and the EVA/clay composites. During the second step, the degradation behavior of EVA, EVA/clay and EVA/organoclay composites in air is very similar to that in nitrogen, however the degradation temperature was 13, 25 and 14 °C lower than that in air with nitrogen, respectively.

TABLE IV The TGA results of EVA, EVA/MMT (95/5) and EVA/ODA-MMT (95/5) composites in air

Sample	T_I^i (°C)	T_{II}^i (°C)	T_{II}^{max} (°C)
EVA	245	426	434
EVA/MMT	287	430	438
EVA/ODA-MMT	296	448	476

The nanocomposites showed an effect of protection and stabilization towards the thermo-oxidation in air, which might be derived from the barrier effect of the diffusion of both the volatile thermo-oxidation products to the gas phase and oxygen from the gas to the polymer matrix [10, 12]. The barrier effect increased because of the ablative reassembling of the silicate layers on the polymer surface during the process of volatilization [14, 15].

References

1. Y. KOJIMA, A. USUKI, M. KAWASUMI *et al., J. Mater. Res.* **8** (1993) 1185.
2. Y. KE, C. LONG and Z. QI, *J. Appl. Polym. Sci.* **71** (1999) 1139.
3. L. LIU, Z. QI and X. ZHU, *ibid.* **71** (1999) 1133.
4. P. B. MESSERSMITH and E. P. GIANNELIS, *J. Polym. Sci. Polym. Chem. Edt.* **33** (1995) 1047.
5. A. AKELAH and A. MOET, *J. Mater. Sci.* **31** (1996) 3589.
6. Y. KOJIMA, A. USUKI, M. KAWASUMI *et al., J. Appl. Polym. Sci.* **49** (1993) 1259.
7. J. W. GILMAN, T. KASHIWAGI and J. D. LICHTENHAN, *SAMPE. J.* **33** (1997) 40.
8. R. A. VAIA, G. PRICE, P. N. RUTH *et al., J. Appl. Clay. Sci.* **15** (1999) 67.
9. M. ZANETTI, G. CAMINO and R. MULHAUPT, *Polym. Degrad. Stab.* **74** (2001) 413.
10. M. ZANETTI, G. CAMINO, R. THOMANN *et al., Polymer* **42** (2001) 4501.
11. A. RIVA, M. ZANETTI, M. BRAGLIA *et al., Polym. Degrad. Stab.* **77** (2002) 299.
12. Y. TANG, Y. HU, S. F. WANG *et al., ibid.* **78** (2002) 555.
13. M. ALEXANDRE, G. BEYER, C. HENRIST *et al., Chem. Mater.* **13** (2001) 3830.
14. M. ZANETTI, T. KASHIWAGI, L. FALQUI *et al., ibid.* **14** (2002) 881.
15. J. W. GILMAN, C. L. JACKSON, A. B. MORGAN *et al., ibid.* **12** (2000) 1866.

Received 31 December 2003
and accepted 3 February 2004